

# Identification of a serotonin/glutamate receptor complex implicated in psychosis

Javier González-Maeso<sup>1,2</sup>, Rosalind L. Ang<sup>1</sup>, Tony Yuen<sup>1</sup>, Pokman Chan<sup>1</sup>, Noelia V. Weisstaub<sup>5,6</sup>, Juan F. López-Giménez<sup>8</sup>, Mingming Zhou<sup>5</sup>, Yuuya Okawa<sup>1</sup>, Luis F. Callado<sup>9,10</sup>, Graeme Milligan<sup>8</sup>, Jay A. Gingrich<sup>5,6,7</sup>, Marta Filizola<sup>3</sup>, J. Javier Meana<sup>9,10</sup> & Stuart C. Sealfon<sup>1,4</sup>

The psychosis associated with schizophrenia is characterized by alterations in sensory processing and perception<sup>1,2</sup>. Some antipsychotic drugs were identified by their high affinity for serotonin 5-HT<sub>2A</sub> receptors (2AR)<sup>3,4</sup>. Drugs that interact with metabotropic glutamate receptors (mGluR) also have potential for the treatment of schizophrenia<sup>5–7</sup>. The effects of hallucinogenic drugs, such as psilocybin and lysergic acid diethylamide, require the 2AR<sup>8–10</sup> and resemble some of the core symptoms of schizophrenia<sup>10–12</sup>. Here we show that the mGluR2 interacts through specific transmembrane helix domains with the 2AR, a member of an unrelated G-protein-coupled receptor family, to form functional complexes in brain cortex. The 2AR–mGluR2 complex triggers unique cellular responses when targeted by hallucinogenic drugs, and activation of mGluR2 abolishes hallucinogen-specific signalling and behavioural responses. In post-mortem human brain from untreated schizophrenic subjects, the 2AR is upregulated and the mGluR2 is downregulated, a pattern that could predispose to psychosis. These regulatory changes indicate that the 2AR–mGluR2 complex may be involved in the altered cortical processes of schizophrenia, and this complex is therefore a promising new target for the treatment of psychosis.

The 2AR and mGluR2/3 show an overlapping distribution in brain cortex in autoradiography studies<sup>13</sup>. The mGluR2 and mGluR3 are not distinguished by autoradiographic ligands. We used fluorescent *in situ* hybridization (FISH) to determine whether either of these receptor subtypes is co-expressed by the same neurons. In layer V mouse somatosensory cortex (SCx), cells positive for 2AR mRNA were mostly positive for *mGluR2* mRNA. The level of expression in SCx was much lower for *mGluR3* mRNA, which rarely co-localized with 2AR mRNA (Fig. 1a). Control studies validated the sensitivity and specificity of the assay, and similar 2AR–mGluR2 mRNA co-localization was found in cortical primary cultures (Fig. 1a–c and Supplementary Fig. 1). Translation of 2AR protein in cortical pyramidal neurons was found to be necessary for normal mGluR2 expression. Mice with globally disrupted 2AR expression (*htr2A*<sup>−/−</sup> mice) showed reduced cortical mGluR2 binding and expression, whereas mice in which 2AR expression had been selectively restored in cortical pyramidal neurons<sup>8,14</sup> showed expression levels equal to those in the control (Supplementary Table 1 and Supplementary Fig. 2). The effects of mGluR2/3 activation on 2AR responses have generally been attributed to synaptic mechanisms<sup>5,6,13,15</sup>. However, the co-localization of 2AR and *mGluR2* and the decrease in mGluR2 expression levels in *htr2A*<sup>−/−</sup> mice led us to examine whether a direct mechanism contributed to cortical cross-talk between these two receptor systems.

Recent studies have demonstrated that some G-protein-coupled receptors (GPCRs) belonging to the same sequence classes can form dimers<sup>16</sup> or, potentially, higher-order oligomers<sup>17</sup>. Although the 2AR and mGluR2 belong to different GPCR classes, we established the existence of 2AR–mGluR2 heterocomplexes by several methods: co-immunoprecipitation of human brain cortex samples (Fig. 1d) and of HEK-293 cells transfected with epitope-tagged receptors (Fig. 2b), bioluminescence resonance energy transfer (BRET) (Fig. 1e and Supplementary Fig. 3), and fluorescence resonance energy transfer (FRET) (Fig. 2d) studies in transfected cells.

To determine whether the formation of the 2AR–mGluR2 complex has functional consequences, we first examined, in mouse SCx membranes, the effects of an mGluR2/3 agonist on the competition binding of several hallucinogenic 2AR agonists (Fig. 1f, top) and of a 2AR agonist on the competition binding of several mGluR2/3 agonists (Fig. 1f, bottom). The agonist affinities for the 2AR and mGluR2/3 were decreased when receptor–G-protein complexes were uncoupled by GTP-γS (Supplementary Fig. 4 and Supplementary Tables 2 and 3). The glutamate agonist LY379268 increased the affinity of all three hallucinogens studied for the 2AR-binding site. Furthermore, the 2AR agonist DOI (1-(2,5-dimethoxy-4-iodophenyl)-2-aminopropane) decreased the affinity of the three mGluR2/3 agonists for the glutamate-receptor-binding site. The allosteric interactions observed were eliminated by antagonist for each modulator (see Supplementary Tables 2 and 3 and Supplementary Fig. 4 for additional concentrations of DOI and LY379268 and for the elimination of the allosteric effects by antagonists). Although the glutamate agonists studied do not distinguish between the mGluR2 and mGluR3 subtypes<sup>18</sup>, the rarity of *mGluR3* and 2AR mRNA co-expression in cortex, the absence of evidence for 2AR–mGluR3 complex formation by co-immunoprecipitation, BRET and FRET, and the detection of 2AR–mGluR2 complexes by these same assays all indicate that the cross-talk identified results from 2AR–mGluR2 complexes.

The differences in the capacity of the mGluR2 and mGluR3 to interact with the 2AR and their close sequence similarity provided the basis for identifying the specific mGluR2 domains responsible for heterocomplex formation. A study of a series of molecular chimaeras of the mGluR2 and mGluR3 (see Fig. 2a) demonstrated that the segment containing transmembrane (TM) helices 4 and 5 of the mGluR2 receptor was both necessary and sufficient for the formation of a complex with the 2AR. The mGluR3 receptor chimaera containing only this segment from the mGluR2 (mGluR3ΔTM4,5) was capable of co-immunoprecipitating with the 2AR (Fig. 2b), mediating

<sup>1</sup>Department of Neurology, <sup>2</sup>Department of Psychiatry, <sup>3</sup>Department of Structural and Chemical Biology and <sup>4</sup>Center for Translational Systems Biology, Mount Sinai School of Medicine, New York, New York 10029, USA. <sup>5</sup>Department of Psychiatry, <sup>6</sup>Sackler Institute Laboratories and <sup>7</sup>Lieber Center for Schizophrenia Research, Columbia University, and the New York State Psychiatric Institute, New York, New York 10032, USA. <sup>8</sup>Division of Biochemistry and Molecular Biology, Institute of Biomedical and Life Sciences, University of Glasgow, Glasgow G12 8QQ, UK. <sup>9</sup>CIBER of Mental Health, and <sup>10</sup>Department of Pharmacology, University of the Basque Country, E-48940 Leioa, Bizkaia, Spain.

allosteric cross-talk (Fig. 2c) and maintaining close proximity with the 2AR as indicated by FRET (Fig. 2d). In contrast, mGluR2ΔTM4,5 did not show evidence of complex formation with the 2AR (Fig. 2, Supplementary Figs 5 and 6, and Supplementary Tables 4 and 5 show complete curves, analysis and evidence of membrane expression of all chimaeras). The absolute and relative levels of expression of heterologous constructs were comparable to the physiological levels found in mouse SCx, and in cortical primary cultures (Supplementary Fig. 5 and Supplementary Table 4). Our data do not exclude the possibility that the predicted 2AR–mGluR2 heterodimer, a model of which is shown in Fig. 2f, assembles into tetramers or larger receptor oligomers<sup>19,20</sup>.

The changes in high-affinity binding caused by 2AR–mGluR2 cross-talk suggested that this complex may serve to integrate serotonin and glutamate signalling and modulate G-protein coupling<sup>21,22</sup>. This hypothesis was tested by measuring the regulation of  $G_{\alpha_{q/11}}$  and

$G_{\alpha_i}$  proteins by 2AR. High-affinity activation of  $G_{\alpha_{q/11}}$  by the 2AR was decreased by co-expression of mGluR2 (Fig. 2e and Supplementary Table 6). The activation of  $G_{\alpha_i}$  by the 2AR was markedly enhanced by mGluR2 co-expression (Fig. 2e and Supplementary Table 7). The mGluR2-dependent effects on both  $G_{\alpha_{q/11}}$  and  $G_{\alpha_i}$  regulation by the 2AR were reversed in the presence of mGluR2 agonist (Fig. 2e and Supplementary Tables 6 and 7). Consonant with the results from co-immunoprecipitation, allosteric modulation and FRET, the functional assays of G-protein activity also show that the TM4–5 segment of the mGluR2, when substituted into the mGluR3, was sufficient for signalling cross-talk to occur (Fig. 2e). These data support the presence of functional and physiological 2AR–mGluR2 complexes that integrate serotonin and glutamate neurotransmission to specify the pattern of G-protein regulation.

Similar evidence for specification of G-protein subtype regulation was also observed for the endogenous brain 2AR–mGluR2 complex

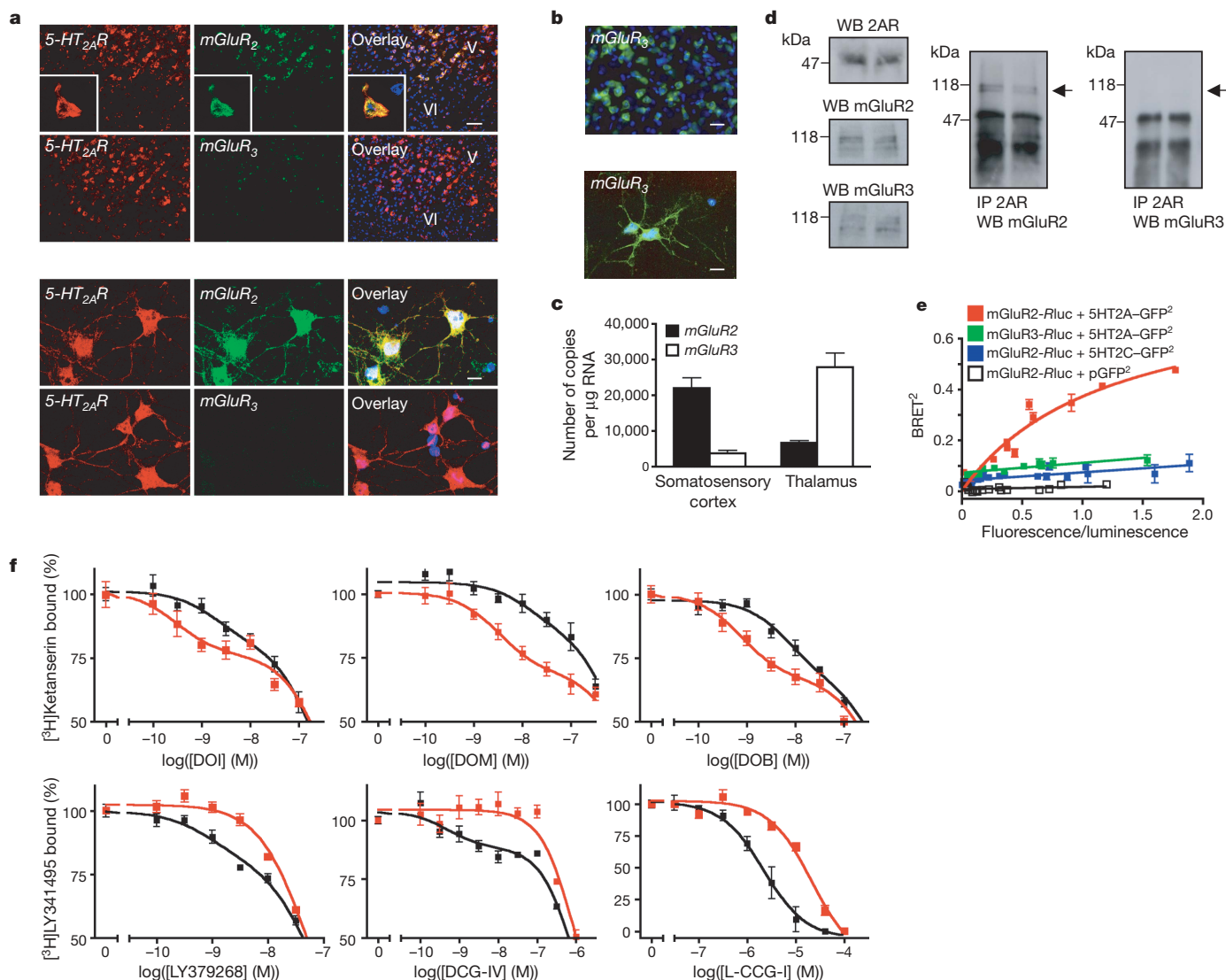


**Figure 1 | 2AR and mGluR2 co-localize and interact.** **a**, 2AR and mGluR2, but not mGluR3, are co-expressed in cortical neurons. Top, mouse somatosensory cortex; bottom, mouse cortical primary culture. Scale bars, 50 μm (top) and 10 μm (bottom). Nuclei are blue. Inset: co-expressing neuron. **b**, FISH for mGluR3 in thalamus. Top, mouse thalamus; bottom, thalamic primary culture. Scale bars, 25 μm (top) and 10 μm (bottom). **c**, mRNA levels measured by real-time PCR (Error bars show s.e.m.; n = 6 per group). **d**, Specific co-immunoprecipitation of 2AR and mGluR2 in duplicate human frontal cortex samples (arrows). WB, western blot; IP, immunoprecipitation. **e**, BRET2 shows specific 2AR and mGluR2

interaction in HEK-293 cells. Data are means ± s.e.m. (n = 3). The mGluR2/2AR curve is fitted better by a saturation curve than by a linear regression, F test (P < 0.001). The other co-transfection data sets show linear regressions. **f**, Top, [<sup>3</sup>H]ketanserin displacement curves in mouse SCx membranes. 2AR agonist affinities were higher in the presence of the mGluR2/3 agonist LY379268 at 10 μM (red) than in vehicle alone (black). [<sup>3</sup>H]LY341495 displacement curves (bottom panels). mGluR2/3 agonist affinities were lower in the presence of the 2AR agonist DOI at 10 μM (red) than in vehicle alone (black). DCG-IV, (2S,2'R,3'R)-2-(2',3'-dicarboxycyclopropyl)-glycine; L-CCG-I, (2S,1'S,2'S)-2-(carboxycyclopropyl)-glycine.

with membranes from cortical primary cultures (Fig. 3a). The pattern of G-protein regulation in cortical pyramidal neurons has been shown to predict specific behavioural responses to 2AR agonists. Hallucinogenic drugs and non-hallucinogenic drugs activate the same population of 2ARs in cortical pyramidal neurons but differ in the 2AR-dependent pattern of G-protein regulation and gene induction that they elicit<sup>8,9</sup>. In brain cortical neurons, the signalling elicited by hallucinogenic and non-hallucinogenic 2AR agonists causes the induction of *c-fos* and requires  $G_{q/11}$ -dependent activation of phospholipase C. However, the signalling of hallucinogens such as DOI and lysergic acid diethylamide (LSD) acting at the 2AR also induces *egr-2*, which is  $G_{i/o}$ -dependent. Thus, *c-fos* expression results from any 2AR signalling, and *egr-2* induction is a specific marker for hallucinogen signalling through the 2AR<sup>8,9</sup>. The finding that mGluR2 modulates the coupling of the 2AR to  $G_i$  (Fig. 3a and Supplementary Tables 6 and 7) indicated that this complex might

be important for hallucinogen signalling. The induction of *c-fos* by hallucinogenic 2AR agonists or by structurally similar non-hallucinogenic 2AR agonists *in vivo* in mouse SCx and in cortical primary cultures (Fig. 3b and Supplementary Figs 8–10) was not affected by the mGluR2/3 agonist LY379268. In contrast, the hallucinogen-specific induction of *egr-2* was selectively blocked by LY379268 in both mouse cortex *in vivo* and in primary cortical cultures (Fig. 3b and Supplementary Figs 8–10 show FISH results with LSD treatment, and real-time PCR gene assay results with DOI, DOM (1-(2,5-dimethoxy-4-methylphenyl)-2-aminopropane), DOB (1-(2,5-dimethoxy-4-bromophenyl)-2-aminopropane), LSD, lisuride hydrogen maleate and ergotamine). We also studied the effects of LY379268 on the head-twitch response behaviour, which is hallucinogen-specific<sup>8,9</sup>. In a similar manner to its effects on G-protein activation and gene induction, the glutamate agonist LY379268 suppressed the induction of the head-twitch response by either DOI or LSD (Supplementary Fig. 11). These results suggest that LY379268 acts at the 2AR–mGluR2 complex to reduce the hallucinogen-specific  $G_{i/o}$  signalling and behaviour. To establish further the functional relevance of 2AR–mGluR2 cross-talk, we compared the responses to the mGluR2/3 antagonist LY341494 in *htr2A*<sup>+/+</sup> and *htr2A*<sup>-/-</sup> mice. The locomotor and vertical activities elicited by LY341494 were significantly attenuated in the *htr2A*<sup>-/-</sup> mice (Fig. 3c), supporting the functional relevance of the 2AR–mGluR2 complex *in vivo* and suggesting that it also influences the endogenous response to glutamate.

The findings that  $G_{i/o}$  regulation, which is necessary for the effects of hallucinogens<sup>8</sup>, is enhanced by the formation of the 2AR–mGluR2 complex and that activation of the mGluR2 component suppresses hallucinogen-specific signalling implicate this complex in the effects of hallucinogens. The neuropsychological effects of hallucinogenic drugs present commonalities with the psychosis of schizophrenia, and both conditions are accompanied by disruptions of cortical sensory processing<sup>10,11,23–27</sup>. We investigated whether the components of the 2AR–mGluR2 signalling complex are dysregulated in the brain cortex of subjects with schizophrenia. We determined the density of binding sites for 2AR and for mGluR2/3 in cortex from schizophrenic subjects and in controls who were matched by gender, age and post-mortem delay (Supplementary Tables 8 and 9). The receptor densities in cortical membranes from untreated schizophrenic subjects were significantly altered, showing increased 2AR levels and decreased mGluR2/3 levels (Fig. 4a, b). mRNA assays showed that expression of *mGluR2* but not *mGluR3* was decreased in cortex from schizophrenic subjects (Fig. 4e). The studies in mouse show that

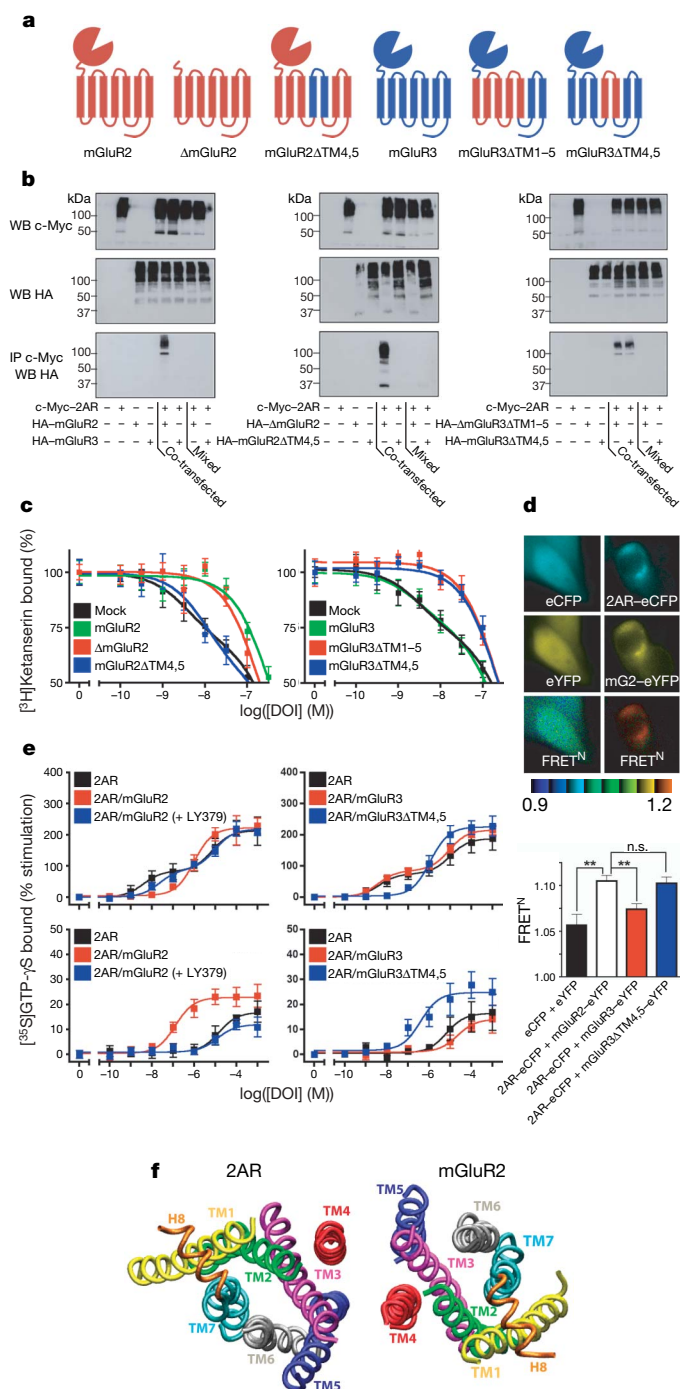


**Figure 2 | mGluR2 transmembrane domains 4/5 mediate association with 2AR.** **a**, mGluR2/mGluR3 chimaeras studied. **b**, c-Myc-2AR and haemagglutinin (HA)-mGluR2/mGluR3 chimaera co-immunoprecipitations. Cells separately expressing each construct were also mixed. WB, western blot; IP, immunoprecipitation. **c**, 2AR competition binding in cells stably expressing the 2AR and transfected with mGluR2/mGluR3 chimaeras. Error bars show s.e.m. ( $n = 4$ ). **d**, FRET in cells expressing 2AR tagged with enhanced cyan fluorescent protein (eCFP) and either mGluR2, mGluR3 or mGluR3 $\Delta$ TM4,5 chimaera, all tagged with enhanced yellow fluorescent protein (eYFP). Pseudocolour images represent normalized values (FRET<sup>N</sup>). Numbers of samples: eCFP + eYFP,  $n = 19$ ; 2AR-eCFP + mGluR2-eYFP,  $n = 43$ ; 2AR-eCFP + mGluR3-eYFP,  $n = 31$ ; 2AR-eCFP + mGluR3 $\Delta$ TM4,5-eYFP,  $n = 27$ . Two asterisks,  $P < 0.01$ ; analysis of variance with Dunnett's post hoc test. n.s., not significant. Error bars show s.e.m. **e**, DOI-stimulated [<sup>35</sup>S]GTP- $\gamma$ S binding in membranes followed by immunoprecipitation with anti- $G_{q/11}$  (top) or anti- $G_{i1,2,3}$  (bottom). Cells stably expressing 2AR were transfected with mGluR2, mGluR3 or mGluR3 $\Delta$ TM4,5. The potency of DOI activating  $G_{q/11}$  was significantly increased when the 2AR was co-expressed with either mGluR2 or mGluR3 $\Delta$ TM4,5, an effect abolished by 10  $\mu$ M LY379268 (LY379) ( $P < 0.001$  by  $F$  test). Data are means  $\pm$  s.e.m. for three experiments performed in triplicate. **f**, Ribbon backbone representation of the transmembrane helices of the 2AR–mGluR2 heteromer model, seen from the intracellular face.



activation of the mGluR2 component of the 2AR–mGluR2 complex eliminates the hallucinogen-specific component of the signalling responses to LSD-like drugs. Thus, the increased 2AR and decreased mGluR2 found in the brain in schizophrenia may predispose to a hallucinogenic pattern of signalling.

Many laboratories have attempted to determine the density of 2AR in post-mortem brain from subjects with schizophrenia, and some studies have reported decreased or unchanged 2AR densities<sup>28</sup>. To try to understand the basis for these discrepancies from our results, we first studied the effects of chronic antipsychotic treatment on the 2AR and mGluR2 in mouse. The chronic atypical antipsychotic clozapine specifically downregulated the level of expression of 2AR and of mGluR2 in mouse SCx (Supplementary Fig. 12). The downregulation

of mGluR2 by clozapine required expression of the 2AR, because it did not occur in *htr2A*<sup>-/-</sup> mice (Supplementary Fig. 12) and was not induced by the chronic typical antipsychotic haloperidol (Supplementary Fig. 13). In concordance with the effects of clozapine in murine models, the density of 2AR was reduced to control levels in postmortem human brain cortex of schizophrenics treated with atypical antipsychotic drugs (Fig. 4c), and the mGluR2/3-binding sites were also downregulated (Fig. 4d). The onset of psychosis in schizophrenia usually occurs in later adolescence or early adulthood<sup>1</sup>. We studied the relationship of receptor densities with ageing: both [<sup>3</sup>H]ketanserin and [<sup>3</sup>H]LY341495 binding showed a highly significant negative correlation with age (Supplementary Fig. 14). Hallucinations and delusions typically attenuate with ageing<sup>29</sup>, which correlates with the lower density of the components of the 2AR–mGluR2 complex that we observed in older subjects. Consequently, the marked dysregulation of both 2AR and mGluR2 expression in schizophrenia would be unlikely to be observed in samples from heterogeneous groups including treated patients<sup>28</sup> or in studies including older patients<sup>28,30</sup>.

These studies identify the 2AR–mGluR2 complex as a possible site of action of hallucinogenic drugs. The glutamate and serotonin systems have both been implicated in psychotic disorders, and the components of this complex are found to be differentially regulated in cortex from individuals with schizophrenia. Our results are consistent with the hypothesis that the 2AR–mGluR2 complex integrates serotonin and glutamate signalling to regulate the sensory gating functions of the cortex, a process that is disrupted in psychosis.

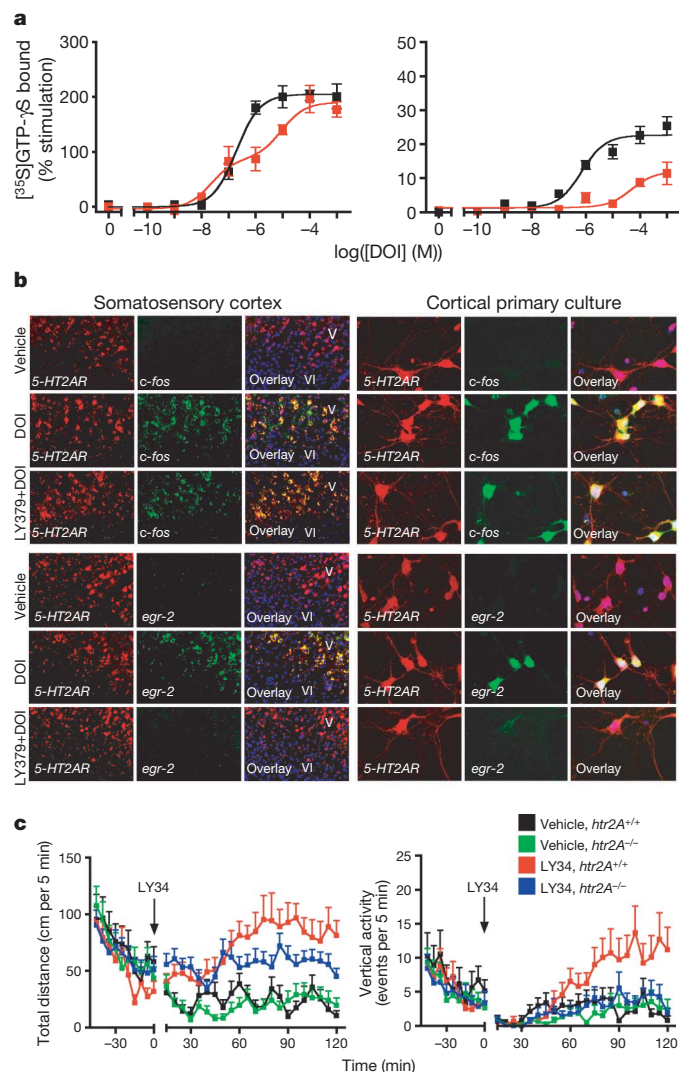


**Figure 3 | 2AR–mGluR2 complex-dependent modulation of cellular and behavioural responses.** **a**, DOI-stimulated [<sup>35</sup>S]GTP-γS binding in primary culture membranes followed by immunoprecipitation with anti-Gα<sub>q/11</sub> antibodies (left) or anti-Gα<sub>i1,2,3</sub> antibodies (right). DOI Gα<sub>i1,2,3</sub> activation potency was significantly decreased by 10 μM LY379268 (red) compared with vehicle alone (black). Data are mean ± s.e.m. for three experiments performed in triplicate. **b**, FISH in mice injected with vehicle or 2 mg kg<sup>-1</sup> DOI 15 min after injection with vehicle or 15 mg kg<sup>-1</sup> LY379268 (left), and in primary cultures treated with 10 μM DOI 15 min after being pretreated with vehicle or 10 μM LY379268 (right). Nuclei are blue. Scale bars, 50 μm. **c**, Distance and vertical activity induced in *htr2A*<sup>+/+</sup> and *htr2A*<sup>-/-</sup> mice by the mGluR2/3 antagonist LY341495 (LY34) at 6 mg kg<sup>-1</sup>. In *htr2A*<sup>-/-</sup> mice, the effect of LY341495 on distance was decreased ( $P < 0.05$ ; Bonferroni's post hoc test of two-factor analysis of variance), and its effect on vertical activity was absent ( $n = 30–32$ ). Error bars show s.e.m.

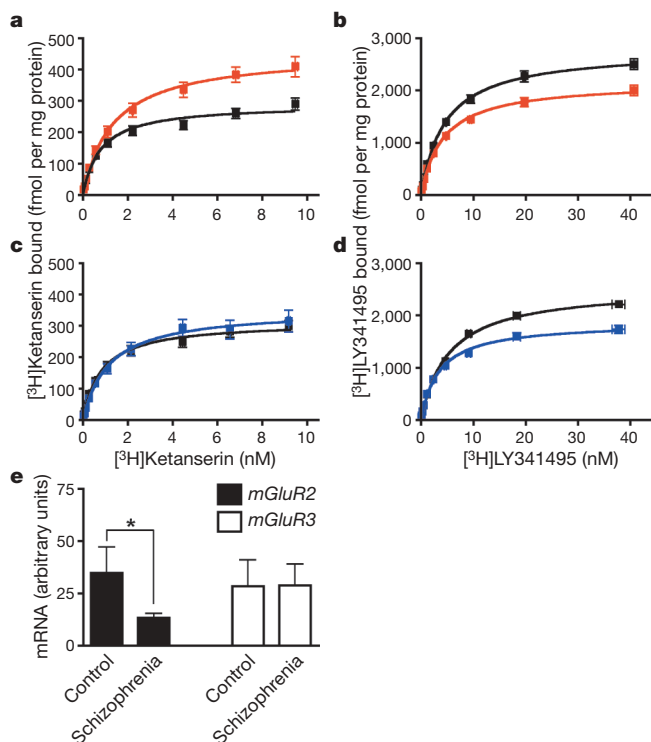


**Figure 4 | 2AR is increased and mGluR2 is decreased in schizophrenia.**

**a, b**, Frontal cortex membrane receptor binding assays from untreated schizophrenic subjects (red;  $n = 13$ ) and matched control subjects (black;  $n = 13$ ). In schizophrenia, [<sup>3</sup>H]ketanserin binding (**a**) was higher and [<sup>3</sup>H]LY341495 binding (**b**) was lower ( $P < 0.05$ ; Student's *t*-test). Error bars show s.e.m. **c, d**, Receptor binding in antipsychotic-treated schizophrenic subjects (blue;  $n = 12$ ) and matched control subjects (black;  $n = 12$ ). In treated schizophrenia, [<sup>3</sup>H]ketanserin binding (**c**) was unaffected and [<sup>3</sup>H]LY341495 binding (**d**) was lower ( $P < 0.05$ ). Error bars show s.e.m. **e**, *mGluR2* mRNA expression is decreased in untreated schizophrenic subjects ( $n = 7$ ) compared with matched control subjects ( $n = 7$ ; asterisk,  $P < 0.05$ ; error bars show s.e.m.).

## METHODS SUMMARY

All reagents were purchased from commercial vendors except for LY379268 (Eli Lilly and Co.). Mouse lines, treatment protocols, behavioural studies, dissections, and primary neuronal cultures, approved by Institutional Use and Care Committees, have been described previously<sup>8,9</sup>. Protocols used for FISH<sup>8</sup>, binding assays<sup>8</sup>, real-time PCR<sup>8</sup>, FRET<sup>17</sup> and co-immunoprecipitation<sup>17</sup> were performed as described previously or with minor modifications. Epitope-tagged, BRET2, FRET and chimaera receptor constructs were generated by using standard cloning techniques and were confirmed by sequencing. BRET2 using *Renilla* luciferase and green fluorescent protein (GFP2) was performed in HEK-293 cells. Matched schizophrenia and control human brains were obtained from autopsies performed in the Basque Institute of Legal Medicine, Bilbao, Spain, in compliance with policies of research and ethical review boards for post-mortem brain studies.

**Full Methods** and any associated references are available in the online version of the paper at [www.nature.com/nature](http://www.nature.com/nature).

**Received 2 November; accepted 20 December 2007.**

**Published online 24 February 2008.**

- Freedman, R. Schizophrenia. *N. Engl. J. Med.* **349**, 1738–1749 (2003).
- Sawa, A. & Snyder, S. H. Schizophrenia: diverse approaches to a complex disease. *Science* **296**, 692–695 (2002).
- Lieberman, J. A. et al. Serotonergic basis of antipsychotic drug effects in schizophrenia. *Biol. Psychiatry* **44**, 1099–1117 (1998).
- Miyamoto, S., Duncan, G. E., Marx, C. E. & Lieberman, J. A. Treatments for schizophrenia: a critical review of pharmacology and mechanisms of action of antipsychotic drugs. *Mol. Psychiatry* **10**, 79–104 (2005).
- Aghajanian, G. K. & Marek, G. J. Serotonin model of schizophrenia: emerging role of glutamate mechanisms. *Brain Res. Brain Res. Rev.* **31**, 302–312 (2000).
- Marek, G. J. Metabotropic glutamate 2/3 receptors as drug targets. *Curr. Opin. Pharmacol.* **4**, 18–22 (2004).
- Patil, S. T. et al. Activation of mGlu2/3 receptors as a new approach to treat schizophrenia: a randomized Phase 2 clinical trial. *Nature Med.* **13**, 1102–1107 (2007).
- Gonzalez-Maeso, J. et al. Hallucinogens recruit specific cortical 5-HT<sub>2A</sub> receptor-mediated signaling pathways to affect behavior. *Neuron* **53**, 439–452 (2007).
- Gonzalez-Maeso, J. et al. Transcriptome fingerprints distinguish hallucinogenic and nonhallucinogenic 5-hydroxytryptamine 2A receptor agonist effects in mouse somatosensory cortex. *J. Neurosci.* **23**, 8836–8843 (2003).
- Vollenweider, F. X., Vollenweider-Scherpenhuyzen, M. F., Babler, A., Vogel, H. & Hell, D. Psilocybin induces schizophrenia-like psychosis in humans via a serotonin-2 agonist action. *Neuroreport* **9**, 3897–3902 (1998).
- Gouzoulis-Mayfrank, E. et al. Psychological effects of (S)-ketamine and N,N-dimethyltryptamine (DMT): a double-blind, cross-over study in healthy volunteers. *Pharmacopsychiatry* **38**, 301–311 (2005).
- Colpaert, F. C. Discovering risperidone: the LSD model of psychopathology. *Nature Rev. Drug Discov.* **2**, 315–320 (2003).
- Marek, G. J., Wright, R. A., Schoepp, D. D., Monn, J. A. & Aghajanian, G. K. Physiological antagonism between 5-hydroxytryptamine<sub>2A</sub> and group II metabotropic glutamate receptors in prefrontal cortex. *J. Pharmacol. Exp. Ther.* **292**, 76–87 (2000).
- Weisstaub, N. V. et al. Cortical 5-HT<sub>2A</sub> receptor signaling modulates anxiety-like behaviors in mice. *Science* **313**, 536–540 (2006).
- Benneyworth, M. A. et al. A selective positive allosteric modulator of metabotropic glutamate receptor subtype 2 blocks a hallucinogenic drug model of psychosis. *Mol. Pharmacol.* **72**, 477–484 (2007).
- Angers, S., Salahpour, A. & Bouvier, M. Dimerization: an emerging concept for G protein-coupled receptor ontogeny and function. *Annu. Rev. Pharmacol. Toxicol.* **42**, 409–435 (2002).
- Lopez-Gimenez, J. F., Canals, M., Pediani, J. D. & Milligan, G. The  $\alpha 1b$ -adrenoceptor exists as a higher-order oligomer: effective oligomerization is required for receptor maturation, surface delivery, and function. *Mol. Pharmacol.* **71**, 1015–1029 (2007).
- Wright, R. A., Arnold, M. B., Wheeler, W. J., Ornstein, P. L. & Schoepp, D. D. [<sup>3</sup>H]LY341495 binding to group II metabotropic glutamate receptors in rat brain. *J. Pharmacol. Exp. Ther.* **298**, 453–460 (2001).
- Palczewski, K. et al. Crystal structure of rhodopsin: A G protein-coupled receptor. *Science* **289**, 739–745 (2000).
- Fotiadis, D. et al. Atomic-force microscopy: Rhodopsin dimers in native disc membranes. *Nature* **421**, 127–128 (2003).
- Kenakin, T. Efficacy at G-protein-coupled receptors. *Nature Rev. Drug Discov.* **1**, 103–110 (2002).
- Gonzalez-Maeso, J., Rodriguez-Puertas, R. & Meana, J. J. Quantitative stoichiometry of G-proteins activated by  $\mu$ -opioid receptors in postmortem human brain. *Eur. J. Pharmacol.* **452**, 21–33 (2002).
- Carlsson, A. The neurochemical circuitry of schizophrenia. *Pharmacopsychiatry* **39** (Suppl. 1), S10–S14 (2006).
- Vollenweider, F. X. & Geyer, M. A. A systems model of altered consciousness: integrating natural and drug-induced psychoses. *Brain Res. Bull.* **56**, 495–507 (2001).
- Vollenweider, F. X. et al. Positron emission tomography and fluorodeoxyglucose studies of metabolic hyperfrontality and psychopathology in the psilocybin model of psychosis. *Neuropsychopharmacology* **16**, 357–372 (1997).
- Umbrecht, D. et al. Effects of the 5-HT<sub>2A</sub> agonist psilocybin on mismatch negativity generation and AX-continuous performance task: implications for the neuropharmacology of cognitive deficits in schizophrenia. *Neuropsychopharmacology* **28**, 170–181 (2003).
- Gouzoulis-Mayfrank, E. et al. Inhibition of return in the human 5HT<sub>2A</sub> agonist and NMDA antagonist model of psychosis. *Neuropsychopharmacology* **31**, 431–441 (2006).
- Dean, B. The cortical serotonin<sub>2A</sub> receptor and the pathology of schizophrenia: a likely accomplice. *J. Neurochem.* **85**, 1–13 (2003).
- Davidson, M. et al. Severity of symptoms in chronically institutionalized geriatric schizophrenic patients. *Am. J. Psychiatry* **152**, 197–207 (1995).
- Gurevich, E. V. & Joyce, J. N. Alterations in the cortical serotonergic system in schizophrenia: a postmortem study. *Biol. Psychiatry* **42**, 529–545 (1997).

**Supplementary Information** is linked to the online version of the paper at [www.nature.com/nature](http://www.nature.com/nature).

**Acknowledgements** We thank L. Devi and L. Ivic for critiquing the manuscript; S. Morgello and the Manhattan HIV Brain Bank for providing control brain cortex; I. Rodil, L. Uriguen and B. Lin for assistance with biochemical assays; the Mount Sinai Microscopy and Microarray, Real-Time PCR and Bioinformatics Shared Research Facilities; the staff members of the Basque Institute of Legal Medicine for their cooperation in the study; J. H. Prather for a gift of LY379268; and J.-P. Pin for providing the signalling peptide sequence of rat mGluR5. This study was supported by the National Institutes of Health, UPV/EHU and the Basque Government, the Spanish Ministry of Health, the REM-TAP Network, the Whitehall Foundation, the Gatsby Foundation and the American Foundation for Suicide Prevention.

**Author Contributions** J.G.M. and S.C.S. designed experiments, supervised research and wrote the manuscript. J.G.M. performed experiments. R.L.A. performed BRET experiments. T.Y. designed and cloned receptor chimaeras. Y.O. assisted with experiments. P.C. performed FISH studies. N.V.W. and M.Z., supervised by J.A.G., performed behaviour experiments and developed mutant mouse lines. J.L.G., supervised by G.M., performed FRET experiments. M.F. performed computer modelling. L.F.C. and J.J.M. performed schizophrenia post-mortem human brain studies. All authors discussed the results and commented on the manuscript.

**Author Information** Reprints and permissions information is available at [www.nature.com/reprints](http://www.nature.com/reprints). Correspondence and requests for materials should be addressed to J.G.M. (javier.maeso@mssm.edu) or S.C.S. (stuart.sealfon@mssm.edu).

## METHODS

**Materials and drug administration.** DOI, DOM, DOB, LSD and lisuride hydrogen maleate were purchased from Sigma-Aldrich. (1R,4R,5S,6R)-4-Amino-2-oxabicyclo[3.1.0]hexane-4,6-dicarboxylic acid (LY379268) was obtained from Eli Lilly and Co. 2S-2-amino-2-(1S,2S-2-carboxycyclopropan-1-yl)-3-(xanth-9-yl)-propionic acid (LY341495), (2S,2'R,3'R)-2-(2',3'-dicarboxycyclopropyl)-glycine (DCG-IV), (2S,1'S,2'S)-2-(carboxycyclopropyl)-glycine (L-CCG-I), clozapine and haloperidol were obtained from Tocris Cookson Inc. [<sup>3</sup>H]Ketanserin and [<sup>35</sup>S]GTP-γS were purchased from PerkinElmer. [<sup>3</sup>H]LY341495 was purchased from American Radiolabelled Chemicals, Inc. The injected doses (intraperitoneal) were: DOI, 2 mg kg<sup>-1</sup>; DOM, 4 mg kg<sup>-1</sup>; DOB, 1 mg kg<sup>-1</sup>; LSD, 0.24 mg kg<sup>-1</sup>; lisuride hydrogen maleate, 0.4 mg kg<sup>-1</sup>; ergotamine, 0.5 mg kg<sup>-1</sup>; LY379268, 15 mg kg<sup>-1</sup>; LY341495, 6 mg kg<sup>-1</sup>; clozapine, 25 mg kg<sup>-1</sup>; and haloperidol, 1 mg kg<sup>-1</sup>, unless otherwise indicated.

**Transient transfection of HEK-293 cells.** HEK-293 cells were maintained in DMEM medium supplemented with 10% (v/v) fetal bovine serum at 37 °C in a humidified 5% CO<sub>2</sub> atmosphere. Transfection was performed with Lipofectamine 2000 reagent (Invitrogen) in accordance with the manufacturer's instructions. HEK-293 cells stably expressing human 2AR have been described previously<sup>9,31</sup>.

**Co-immunoprecipitation studies.** Co-immunoprecipitation studies in post-mortem human brain, and co-immunoprecipitation studies using an N-terminally c-Myc-tagged form of 2AR, and N-terminally haemagglutinin (HA)-tagged forms of mGluR2, mGluR3 or mGluR2/mGluR3 chimaeras in HEK-293 cells were performed as described previously, with minor modifications<sup>17</sup>. In brief, the samples were incubated overnight with protein A/G beads and anti-2AR (post-mortem human brain) or anti-c-Myc antibody (HEK-293 cells) at 4 °C on a rotating wheel. Equal amounts of proteins were resolved by SDS-PAGE. Detection of proteins by immunoblotting with anti-2AR (Santa Cruz Biotechnology), anti-mGluR2 and anti-mGluR3 (Abcam Inc.) in post-mortem human brain, or anti-c-Myc and anti-HA antibodies (Santa Cruz Biotechnology) in HEK-293 cells was conducted with an enhanced chemiluminescence system in accordance with the manufacturer's recommendations.

**Bioluminescence resonance energy transfer (BRET2) in HEK-293 live cells.** The human 2AR, serotonin 5-HT<sub>2C</sub> (2CR), mGluR2 and mGluR3 receptors with mutated stop codons were subcloned into the pRluc and pGFP<sup>2</sup> plasmids (PerkinElmer), such that *Renilla* luciferase (Rluc) and green fluorescent protein (GFP2) were present at the carboxy termini of the receptors. All sequences were confirmed by DNA sequencing. After 48 h, transfected cells were washed with PBS, suspended to (1–2) × 10<sup>6</sup> cells ml<sup>-1</sup> and were treated with DeepBlueC Coelenterazine Substrate (5 μM final concentration; PerkinElmer). Equivalent amounts of total DNA composed of various ratios of the Rluc- or GFP2-tagged receptors were transfected<sup>32</sup>. Light emission was monitored with a Fusion Universal Microplate Analyser (PerkinElmer). A BRET2 signal is defined as the light emitted by GFP2 at 515 nm in response to the light emitted at 410 nm by Rluc on catalysis of DeepBlueC. The values were corrected by subtracting the background BRET2 signal detected when the receptor–Rluc construct was expressed alone (see Supplementary Fig. 3 for luminescence and fluorescence values). The specificities of mGluR2–Rluc and 2AR–GFP2 interactions were assessed by comparison with co-expression of mGluR2–Rluc and 2CR–GFP2, mGluR3–Rluc and 2AR–GFP2 and mGluR2–Rluc and GFP2. Data from a single experiment, which was replicated three times, are shown as means ± s.e.m. (Fig. 1e).

**FRET.** Forms of the 2AR and mGluR2 C-terminally fused to eCFP and eYFP were generated, and FRET microscopy in living cells was conducted as reported previously<sup>17</sup>. Results from a single experiment, representative of two or three independent studies, are shown in Fig. 2d.

**[<sup>3</sup>H]Ketanserin, [<sup>3</sup>H]LY341495 and [<sup>35</sup>S]GTP-γS binding.** Membrane preparations and [<sup>3</sup>H]ketanserin binding assays were performed as reported previously<sup>8</sup>. [<sup>3</sup>H]LY341495 binding was performed as described previously, with minor modifications<sup>18</sup>. In brief, membrane preparations were incubated for 60 min at 4 °C. Non-specific binding was determined in the presence of 1 mM L-glutamate. [<sup>35</sup>S]GTP-γS binding experiments were initiated by the addition of membranes containing 35 μg of protein to an assay buffer (20 mM HEPES, 3 mM MgCl<sub>2</sub>, 100 mM NaCl, 0.2 mM ascorbic acid and 0.5 nM [<sup>35</sup>S]GTP-γS) supplemented with 0.1 μM or 10 μM GDP for Gα<sub>q/11</sub> and Gα<sub>i</sub>, respectively, and containing the indicated concentration of ligands. Non-specific binding was determined in the presence of 100 μM GTP-γS. Reactions were incubated for 30 min at 30 °C, and were terminated by the addition of 0.5 ml of ice-cold buffer, containing 20 mM HEPES, 3 mM MgCl<sub>2</sub>, 100 mM NaCl and 0.2 mM ascorbic acid. The samples were centrifuged at 16,000g for 15 min at 4 °C, and the resulting pellets were resuspended in solubilization buffer (100 mM Tris, 200 mM NaCl, 1 mM EDTA, 1.25% Nonidet P40) plus 0.2% SDS. Samples were precleared with Pansorbin

(Calbiochem), followed by immunoprecipitation with antibody against Gα<sub>q/11</sub> or Gα<sub>i1,2,3</sub> (Santa Cruz Biotechnology). Finally, the immunocomplexes were washed twice with solubilization buffer, and bound [<sup>35</sup>S]GTP-γS was measured by liquid-scintillation spectrometry.

**Construction of receptor chimaeras.** All PCR reactions were performed with PfuTurbo Hotstart DNA polymerase (Stratagene). Cycling conditions were 30 cycles of 94 °C for 30 s, 55 °C for 30 s and 72 °C for 1 min per kilobase of amplicon, with an initial denaturation/activation of 94 °C for 2 min and a final extension of 72 °C for 7 min.

HA-tagged wild-type human mGluR2 and mGluR3 constructs: the rat mGluR5 signal peptide (SP)<sup>33</sup> along with an HA epitope tag was amplified by PCR with primers *NheI*-HA\_SP/S (5'-TTTgtagctGAATTCCTTCTCTAAATGG-3') and HA\_SP-*KpnI*/A (5'-TTTggtaccACGCGTGGCGTAGTCGG-GTA-3') with pRK5 as template. Wild-type human mGluR2 and mGluR3 were amplified with primers *MluI*-hGRM2/S (5'-agctacgctAAGAAGGTGCTGACCCTGGA-3') hGRM2-*XbaI*/A (5'-AATctagaTCAAAGCGATGACGTTGTGCGAG-3') and *KpnI*-hGRM3/S (5'-acgtggtaccTTAGGGGACCATAACTTCT-3') hGRM3-*XhoI*/A (5'-acgtctcgagTCACAGAGATGAGGTGGTGG-3'), respectively. The rat mGluR5 signal peptide/HA epitope fragment was digested with *NheI* and *MluI*, the human mGluR2 fragment was digested with *MluI* and *XbaI* and were simultaneously subcloned into the *NheI* and *XbaI* sites of pcDNA3.1 (Invitrogen) to yield the HA-tagged mGluR2 construct. Similarly, the rat mGluR5 signal peptide/HA fragment was digested with *NheI* and *KpnI*, the human mGluR2 PCR product was digested with *KpnI* and *XhoI*, and they were subcloned simultaneously into the *NheI* and *XhoI* sites of pcDNA3.1 to give the HA-tagged mGluR2 construct.

Chimaeric human mGluR2 with transmembrane domain 4 and 5 from human mGluR3: a fragment of the transmembrane domain TM1 to the C terminus of the second intracellular loop of the human mGluR2 was amplified with primers hGRM2-1476/S (5'-GGACACACGCTCATCCCAT-3') and hGRM2i2GRM3-TM4/A (5'-CAGATGAAAACCTGAGAACTAGGACTGATGAAGCGTGGCC-3'). A fragment of the TM4 to TM5 of the human mGluR3 was amplified with primers hGRM2i2GRM3TM4/S (5'-GGCCACGCTTCATCAGTCTAGTTC-TCAGGTTTTCATCTG-3') and hGRM3TM5GRM2i3/A (5'-TTTTCGGGG-CACTGCGAGTTTGAAGGCGTACACAGTGC-3'). The two fragments were annealed and reamplified with primers hGRM2-1476/S and hGRM3TM5-GRM2i3/A. The third intracellular loop to the C terminus of the human mGluR2 was amplified with primers hGRM3TM5GRM2i3/S (5'-GCACGTGTG-TACGCCTTCAAACTCGCAAGTGCCCGAAAA-3') and hGRM2-*XbaI*/A. This fragment was then annealed with the previous PCR product and reamplified with primers hGRM2-1476/S and hGRM2-*XbaI*/A. To reconstitute the complete chimaeric receptor, the N-terminal domain of the HA-tagged wild-type human mGluR2 was released with *NheI* and *Bst*BI, the final PCR product was digested with *Bst*BI and *XbaI*, and the two fragments were simultaneously subcloned into the *NheI* and *XbaI* sites of pcDNA3.1.

Chimaeric human mGluR3 with transmembrane domain 4 and 5 from human mGluR2: a fragment of the transmembrane domain TM1 to the C terminus of the second intracellular loop of the human mGluR3 was amplified with primers hGRM3-2541/S (5'-TGAAAGTTGGTCACTGGGCA-3') and hGRM3i2GRM2-TM4/A (5'-CAGATGCGCCACCTGTGAGGCGGGCTGATGAATTTGGCC-3'). A fragment of the TM4 to TM5 of the human mGluR2 was amplified with primers hGRM3i2GRM2TM4/S (5'-GGCCAAAATTCATCAGCCCCGCCTC-ACAGGTGGCCATCTG-3') and hGRM2TM5GRM3i3/A (5'-TTTTCTGGG-CACTTCGCGTCTTGAAGGCATAAAGCGTGC-3'). The two fragments were annealed and reamplified with primers hGRM3-2541/S and hGRM2TM5-GRM3i3/A. The third intracellular loop to the C terminus of the human mGluR3 was amplified with primers hGRM2TM5GRM3i3/S (5'-GCACGC-TTATGCCTTCAAGACGCGGAAGTGCCAGAAAA-3') and hGRM3-*XhoI*/A. This fragment was then annealed with the previous PCR product and reamplified with primers hGRM3-2541/S and hGRM3-*XhoI*/A. To reconstitute the complete chimaeric receptor, the N-terminal domain of the HA-tagged wild-type human mGluR3 was released with *NheI* and *Pst*I, the final PCR product was digested with *Pst*I and *XhoI*, and the two fragments were simultaneously subcloned into the *NheI* and *XhoI* sites of pcDNA3.1.

Chimaeric human mGluR3 with transmembrane domains 1 to 5 from human mGluR2: a small fragment of the N-terminal domain to the beginning of TM1 of the human mGluR3 was amplified with primers hGRM3-2541/S and hGRM3-NGRM2TM1/A (5'-ACAGCCCAGGCATCGCCCCAGCGGATGTAGTCCTC-CAGGAAGT-3'). A fragment of the TM1 to TM5 of the human mGluR2 was amplified with primers hGRM3NGRM2TM1/S (5'-ACCTTCCTGAG-GACTACATCCGCTGGGGCGATGCCTGGGCTGT-3') and hGRM2TM5-GRM3i3/A. The two fragments were annealed and reamplified with primers hGRM3-2541/S and hGRM2TM5GRM3i3/A. The third intracellular loop to the C terminus of the human mGluR3 was amplified with primers



hGRM2TM5GRM3i3/S and hGRM3-XhoI/A. This fragment was then annealed with the previous PCR product and reamplified with primers hGRM3-2541/S and hGRM3-XhoI/A. To reconstitute the complete chimaeric receptor, the N-terminal domain of the HA-tagged wild-type human mGluR3 was released with *NheI* and *PstI*, the final PCR product was digested with *PstI* and *XhoI*, and the two fragments were simultaneously subcloned into the *NheI* and *XhoI* sites of pcDNA3.1.

**Molecular modelling.** Three-dimensional molecular models of the seven TM regions of 2AR and mGluR2 were built by using the crystal structures of  $\beta_2$ -adrenergic receptor<sup>34</sup> and rhodopsin<sup>35</sup>, respectively, as structural templates, and the latest version of the homology-modelling program MODELLER<sup>36</sup>. The use of the very recent crystal structure of  $\beta_2$ -adrenergic receptor to build a model of 2AR is justified by the higher sequence identity between these two receptors than to rhodopsin; in addition, the suitability of the rhodopsin template to build models of family C GPCRs, which includes the mGluR2, has recently been discussed<sup>37</sup>. The sequence alignment between the transmembrane helices of  $\beta_2$ -adrenergic receptor and 2AR was obtained with BLAST<sup>38</sup>. For mGluR2 we used the same alignment with rhodopsin as described in ref. 37. A multiple alignment of available mGluR2 and mGluR3 sequences was performed with the CLUSTALW program, version 1.81 (ref. 39). Supplementary Fig. 7 shows the details of these sequence alignments in the transmembrane regions. To build a reasonable configuration of the 2AR–mGluR2, we used the TM4,5–TM4,5 configuration deriving from atomic force microscopy of rhodopsin in native disc membranes<sup>40</sup> as a template for the heteromer interface between 2AR and mGluR2. This modelling was obtained with the assistance of the Insight II User Graphical Interface (Accelrys Inc.) on a graphics workstation.

**Neuronal primary culture.** Primary cultures of cortical and thalamic neurons were prepared as described previously<sup>8</sup>.

**Mouse brain samples.** Experiments were performed as described previously<sup>8</sup>.

**FISH.** Synthesis of modified DNA oligonucleotide probes, probe labelling and FISH were performed as described previously<sup>8,41</sup>. See Supplementary Table 10 for oligonucleotide probe sequences.

**Quantitative real-time PCR.** Quantitative real-time PCR experiments were performed as described previously<sup>8</sup>. See Supplementary Tables 11 and 12 for primer pair sequences.

**Behavioural studies.** Behavioural studies were performed as described previously<sup>8,14</sup>. Motor function was assessed with a computerized three-dimensional activity monitoring system (AccuScan Instruments). The activity monitor has 32 infrared sensor pairs, with 16 along each side spaced 2.5 cm apart. The system determines motor activity on the basis of the frequency of interruptions to infrared beams traversing the *x*, *y* and *z* planes. Total distance (cm) travelled and vertical activity were determined automatically from the interruptions of beams in the horizontal and vertical planes, respectively.

**Brain samples.** Human brains were obtained at autopsies performed in the Forensic Anatomical Institute, Bilbao, Spain. The study was developed in compliance with policies of research and ethical review boards for post-mortem brain studies (Basque Institute of Legal Medicine, Spain). Deaths were subjected to retrospective searching for previous medical diagnosis and treatment, using the examiner's information and records of hospitals and mental health centres. After searching of ante-mortem information had been fulfilled, 25 subjects who had met criteria of schizophrenia according to the Diagnostic and Statistical Manual of Mental Disorders (DSM-IV)<sup>42</sup> were selected. A toxicological screening for antipsychotics, other drugs and ethanol was performed on samples of blood, urine, liver and gastric contents. All subjects who were drug-free before death (as revealed by the absence of prescriptions in medical histories) also gave negative results in the toxicological screening. The toxicological assays were performed at

the National Institute of Toxicology, Madrid, Spain, using a variety of standard procedures including radioimmunoassay, enzymatic immunoassay, high-performance liquid chromatography and gas chromatography–mass spectrometry. Controls for the present study were chosen among the collected brains on the basis, whenever possible, of the following cumulative criteria: negative medical information on the presence of neuropsychiatric disorders or drug abuse; appropriate gender, age and post-mortem delay to match each subject in the schizophrenia group; sudden and unexpected death (motor vehicle accidents); and toxicological screening for psychotropic drugs with negative results except for ethanol. Tissue pH was assumed to be an indicator of agonal status<sup>43</sup>. Thus, prolonged terminal hypoxia resulted in low tissue pH. It has been shown that gene expression patterns are strongly dependent on tissue pH. Rapid deaths, associated with accidents, cardiac events or asphyxia, generally resulted in a normal tissue pH with a minor influence on gene expression patterns<sup>44</sup>. All schizophrenic and control subjects showed a sudden and rapid death without a long agonal phase. The tissue storage period before assays did not differ significantly between schizophrenic cases ( $82 \pm 9$  months (mean  $\pm$  s.e.m.)) and controls ( $85 \pm 10$  months (mean  $\pm$  s.e.m.)). Two independent groups of schizophrenic subjects were selected depending on the presence of antipsychotics in the toxicological screening (Supplementary Tables 8 and 9).

31. Ebersole, B. J., Visiers, I., Weinstein, H. & Sealfon, S. C. Molecular basis of partial agonism: orientation of indoleamine ligands in the binding pocket of the human serotonin 5-HT<sub>2A</sub> receptor determines relative efficacy. *Mol. Pharmacol.* **63**, 36–43 (2003).
32. James, J. R., Oliveira, M. I., Carmo, A. M., Iaboni, A. & Davis, S. J. A rigorous experimental framework for detecting protein oligomerization using bioluminescence resonance energy transfer. *Nature Methods* **3**, 1001–1006 (2006).
33. Blahos, J. et al. Extreme C terminus of G protein  $\alpha$ -subunits contains a site that discriminates between G<sub>i</sub>-coupled metabotropic glutamate receptors. *J. Biol. Chem.* **273**, 25765–25769 (1998).
34. Cherezov, V. et al. High-resolution crystal structure of an engineered human  $\beta_2$ -adrenergic G protein-coupled receptor. *Science* **318**, 1258–1265 (2007).
35. Li, J., Edwards, P. C., Burghammer, M., Villa, C. & Schertler, G. F. Structure of bovine rhodopsin in a trigonal crystal form. *J. Mol. Biol.* **343**, 1409–1438 (2004).
36. Sali, A. & Blundell, T. L. Comparative protein modelling by satisfaction of spatial restraints. *J. Mol. Biol.* **234**, 779–815 (1993).
37. Binet, V. et al. Common structural requirements for heptahelical domain function in class A and class C G protein-coupled receptors. *J. Biol. Chem.* **282**, 12154–12163 (2007).
38. Altschul, S. F., Gish, W., Miller, W., Myers, E. W. & Lipman, D. J. Basic local alignment search tool. *J. Mol. Biol.* **215**, 403–410 (1990).
39. Thompson, J. D., Higgins, D. G. & Gibson, T. J. CLUSTAL W: improving the sensitivity of progressive multiple sequence alignment through sequence weighting, position-specific gap penalties and weight matrix choice. *Nucleic Acids Res.* **22**, 4673–4680 (1994).
40. Liang, Y. et al. Organization of the G protein-coupled receptors rhodopsin and opsin in native membranes. *J. Biol. Chem.* **278**, 21655–21662 (2003).
41. Chan, P., Yuen, T., Ruf, F., Gonzalez-Maeso, J. & Sealfon, S. C. Method for multiplex cellular detection of mRNAs using quantum dot fluorescent *in situ* hybridization. *Nucleic Acids Res.* **33**, e161 (2005).
42. American Psychiatric Association. *Diagnostic and Statistical Manual of Mental Disorders* 4th edn (American Psychiatric Association, Washington DC, 1994).
43. Preece, P. & Cairns, N. J. Quantifying mRNA in postmortem human brain: influence of gender, age at death, postmortem interval, brain pH, agonal state and inter-lobe mRNA variance. *Brain Res. Mol. Brain Res.* **118**, 60–71 (2003).
44. Li, J. Z. et al. Systematic changes in gene expression in postmortem human brains associated with tissue pH and terminal medical conditions. *Hum. Mol. Genet.* **13**, 609–616 (2004).